

Nonlocality-Reinforced Convolutional Neural Networks for Image Denoising

Cristóvão Cruz, Alessandro Foi, *Senior Member, IEEE*, Vladimir Katkovnik, and Karen Egiazarian, *Fellow, IEEE*

Abstract—We introduce a paradigm for nonlocal sparsity reinforced deep convolutional neural network denoising. It is a combination of a local multiscale denoising by a convolutional neural network (CNN) based denoiser and a nonlocal denoising based on a nonlocal filter (NLF) exploiting the mutual similarities between groups of patches. CNN models are leveraged with noise levels that progressively decrease at every iteration of our framework, while their output is regularized by a nonlocal prior implicit within the NLF. Unlike complicated neural networks that embed the nonlocality prior within the layers of the network, our framework is modular, it uses standard pre-trained CNNs together with standard nonlocal filters. An instance of the proposed framework, called NN3D, is evaluated over large grayscale image datasets showing state-of-the-art performance.

Index Terms—image denoising, convolutional neural network, nonlocal filters, BM3D.

I. INTRODUCTION

Image denoising, one of the most important problems of image processing and computer vision, aims at estimating an unknown image from its noisy observation. Image denoising plays a crucial role at various stages of image processing and can be used as a replacement of explicit image priors: *in pre-processing*, to enhance the output quality and performance of the subsequent image-processing or computer-vision tasks, such as demosaicing, sharpening, compression, object segmentation, classification, and recognition [1]; *in post-processing*: to suppress compression artifacts, such as blocking and ringing [2]; *as plug&play filter*: i.e. as an implicit regularization prior used in various inverse-imaging applications [3] and in end-to-end optimized computational imaging systems [4].

Recently, image denoising received a new boost of interest through the application of advanced machine-learning methods, particularly deep convolutional neural networks (CNNs) [5]. The current most effective image denoising methods can be roughly categorized into *nonlocal filters (NLFs)* (e.g., NLBayes [6], Block Matching 3D (BM3D) [7, 8], and WNNM [9]) or *CNN-based filters (CNNFs)* (e.g., TNRD [10], DnCNN [11]). Their respective advantages and drawbacks are:

Advantages of NLFs: Joint collaborative processing of mutually similar image patches, resulting in superior noise removal where the image exhibits strong self-similarity, such on edges or on regular texture.

This work is supported by the Academy of Finland (projects no. 287150, 2015-2019, and no. 310779, 2017-2021) and European Union's H2020 Framework Programme (H2020-MSCA-ITN-2014) under grant agreement no. 642685 MacSeNet. The authors are with Tampere University of Technology, Finland, and with Noiseless Imaging Ltd, Finland. e-mail: cristovao@noiselessimaging.com

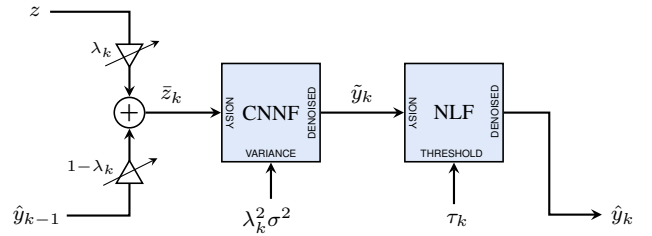


Fig. 1. Flowchart of the generic k -th iteration of the proposed framework. The noisy image z is combined with a previous estimate \hat{y}_{k-1} of the clean image y as the convex combination $\bar{z}_k = \lambda_k z + (1 - \lambda_k) \hat{y}_{k-1}$. First, \bar{z}_k is filtered by a convolutional neural network filter (CNNF); then the CNNF output \hat{y}_k is processed by a Nonlocal filter (NLF), whose output constitutes the new estimate \hat{y}_k . The method iterates with $1 = \lambda_1 > \dots > \lambda_{k-1} > \lambda_k > \dots > 0$.

Drawbacks of NLFs: Inferior performance on pseudo-random textures or singular features, i.e. where the image has weak self-similarity.

This drawback of NLFs is partly overcome through the use of external dictionaries [12], and multi-scale [13, 14], as well as multi-stage iterative approaches [9], which improve the denoising quality by refining the matching of mutually similar blocks and their shrinkage.

Advantages of CNNFs: a) ability to learn and extract complex image features, b) efficient implementation on graphics processing units (GPUs) [5].

Drawbacks of CNNFs: a) learning is very time consuming, from few hours to few days, b) inferior performance on regular textures with high self-similarity.

There have been some attempts to overcome the above-mentioned drawbacks of CNNFs. In particular, [15] extends DnCNN [11] to a feature-space deep residual learning: an input image is represented by the four subbands of a one-level Haar wavelet decomposition, which serve as the input to DnCNN. Despite an improved performance and partial overcome of the drawback b), the method in [15] is still inferior to some of the recent NLFs, especially when regarding to texture [9]. Some recent publications consider a mixture of NLFs and CNNs to improve the performance on images containing self-similar patches. The deep CNN architecture [16] combines explicit patch grouping with a learned potential function and regularization operator. The so-called block matching convolutional neural network (BMCNN) method [17] is similar, using groups of similar patches as inputs to a denoising CNN. The structure of this approach resembles that of BM3D, but replaces the Wiener filtering stage by a CNN similar to DnCNN.

In this paper, we introduce a paradigm that combines the

advantages of a CNNF and of an NLF through a simple iterative modular framework (Sect. II). Unlike [16] and [17], which involve new CNN architectures to leverage nonlocality, ours is a plug-in approach that uses any generic NLF with any generic CNNF, without need of retraining. Furthermore, we present an instance of the proposed framework, called NN3D (Sect. III), that enables a nonlocal self-similarity prior by means of group-wise filtering. Experiments (Sect. IV) carried out on several image datasets demonstrate NN3D's ability to exceed the results obtained by its respective CNNF and NLF components and achieve state-of-the-art results in image denoising.

II. THE PROPOSED FRAMEWORK

We adopt the usual additive white Gaussian noise (AWGN) observation model:

$$z = y + \eta, \quad \eta(\cdot) \sim \mathcal{N}(0, \sigma^2). \quad (1)$$

The goal is to estimate the unknown noise-free image y from the noisy image z and known noise standard deviation σ .

In the proposed framework, which is summarized by the flowchart in Fig. 1 and detailed in Algorithm 1, the noisy image is iteratively filtered by cascaded CNNF for AWGN removal and NLF for enforcing nonlocal self-similarity.

The rationale of the proposed iterative approach can be explained as follows. The CNNF is biased by the learned mapping of the local features, while the NLF is biased towards nonlocal self-similarity. When operating at high noise levels, the local nature of the CNN coupled with the training on external examples, often leads to *hallucination*, i.e. the introduction of patterns that do not exist in the original signal y . In these circumstances, the NLF becomes especially important as it can smooth out hallucinations that fail to meet the self-similarity prior, as we show in Sect. IV. While on the one hand the NLF can attenuate severe localized artifacts, on the other hand it might also introduce excessive spatial smoothing. The proposed framework counteracts this unwanted smoothing by proceeding iteratively. Specifically, at each iteration k , the input to the filter cascade is a convex combination $\bar{z}_k = \lambda_k z + (1 - \lambda_k) \hat{y}_{k-1}$ of the original input z and of the previous estimate \hat{y}_{k-1} . Hence, a fraction of the noise has to be attenuated by the CNNF, and thus the NLF requires weaker regularization, i.e. a smaller τ_k . The step parameter λ_k controls the rate of progress of the iterative procedure. Thus, both λ_k and τ_k are positive and monotonically decreasing with k ; $\lambda_1 = 1$ as \hat{y}_0 is undefined.

III. NONLOCAL SELF-SIMILARITY PRIOR & NN3D

Here we introduce an instance of the above general framework. We call it NN3D, for cascaded Neural Network and 3D collaborative filter, and it enforces the nonlocal self-similarity prior through the following two distinct phases:

A. Block matching: identify groups of similar patches in z ;

B. NLF filtering: shrink spectra of groups extracted from \hat{y}_k .

Block matching (BM) is executed only once, while the NLF filtering is executed at every iteration.

Algorithm 1 Proposed framework

Require: z	noisy signal
Require: σ	noise standard deviation
Require: K	number of iterations
Require: $\lambda_k, k = 1, \dots, K$	iteration steps
Require: $\tau_k, k = 1, \dots, K$	NLF thresholds
1: for $k = 1$ to K do	
2: $\bar{z}_k = \lambda_k z + (1 - \lambda_k) \hat{y}_{k-1}$	convex combination
3: $\tilde{y}_k = \text{CNNF}(\bar{z}_k, \lambda_k \sigma)$	CNN-based filter
4: $\hat{y}_k = \text{NLF}(\tilde{y}_k, \tau_k)$	Nonlocal filter
5: end for	
6: return \hat{y}_K	return final estimate

A. Block matching

BM is the process by which groups of similar blocks are identified and it is a crucial step of many NLFs [6–9]. Noise negatively impacts the BM; therefore, in NN3D, we do the BM on an estimate of y , in particular, for convenience, we use the output \hat{y}_1 of the CNNF: the result is a look-up table of group coordinates $S = \{S_1, \dots, S_N\}$. Each S_j contains the coordinates of N_2 mutually similar blocks of size $N_1 \times N_1$; S is built in such a way that each pixel in the image is covered by at least one block.

B. NLF filtering

Nonlocal self-similarity is enforced by group-wise processing of \tilde{y}_k based on the look-up table S . Specifically, at each iteration k and for each $S_j \in S$, a group $\tilde{\mathbf{g}}_k^{(j)}$ is the 3D array of size $N_1 \times N_1 \times N_2$ formed by stacking the blocks extracted from \tilde{y}_k at the coordinates specified by S_j .

While in principle $\tilde{\mathbf{g}}_k^{(j)}$ could be filtered by 3D-transform domain shrinkage (akin to BM3D), here the CNNF has already operated spatial smoothing and therefore we perform shrinkage only along the third dimension of the group, with respect to a 1D transform \mathcal{T}_{1D} of length N_2 . The filtered group is

$$\hat{\mathbf{g}}_k^{(j)} = \mathcal{T}_{1D}^{-1} \left(\Upsilon \left(\mathcal{T}_{1D}(\tilde{\mathbf{g}}_k^{(j)}), \tau_k \right) \right), \quad (2)$$

where Υ is the shrinkage operator. Here we define Υ as

$$\Upsilon(q, \tau) = q \frac{q^2}{q^2 + \tau^2}, \quad (3)$$

where the threshold τ controls the regularization strength with respect to the nonlocal similarity; its value depends on the magnitude of the deformations introduced by the CNNF as well as on σ . Overall, the filtering (2) attenuates localised deformations that fail to meet the self-similarity constraint.

The image estimate \hat{y}_k is obtained by returning the block estimates from the filtered group $\hat{\mathbf{g}}_k^{(j)}$ to their original locations S_j , where they are aggregated with group-wise weights reciprocal to the energy of the shrinkage factor in (3):

$$w_k^{(j)} = \left\| \frac{\mathcal{T}_{1D}(\tilde{\mathbf{g}}_k^{(j)})^2}{\mathcal{T}_{1D}(\tilde{\mathbf{g}}_k^{(j)})^2 + \tau^2} \right\|_2^{-2}.$$

The operator Υ can be interpreted as a smoothed firm thresholding [19], or as a Wiener filter that uses q as both the

TABLE I

PSNR (dB) PERFORMANCE OF THE PROPOSED NN3D VS COMPETITIVE STATE-OF-THE-ART METHODS. ITALIC RESULTS IN THE BASELINE WDnCNN FOR $\sigma=75$ INDICATE SCALING OF THE NOISY INPUT BY THE FACTOR 50/75 TO MATCH THE MODEL TRAINED FOR $\sigma=50$.

Dataset	σ	BM3D	DnCNN [11]	NN3D(DnCNN)	FFDNet [18]	NN3D(FFDNet)	WDnCNN [15]	NN3D(WDnCNN)
<i>Set12</i>	30	29.12	29.54	29.66	29.63	29.66	29.91	29.96
	50	26.70	27.19	27.32	27.33	27.39	27.48	27.61
	75	24.90	25.22	25.43	25.51	25.61	<i>25.64</i>	25.81
<i>BSD68</i>	30	27.75	28.36	28.41	28.38	28.37	28.56	28.56
	50	25.63	26.23	26.27	26.30	26.29	26.39	26.42
	75	24.22	24.64	24.71	24.79	24.80	<i>24.85</i>	24.91
<i>Urban100</i>	30	28.75	28.88	29.23	29.06	29.18	29.84	30.04
	50	25.95	26.28	26.63	26.55	26.76	27.08	27.49
	75	23.93	23.99	24.45	24.53	24.81	<i>25.06</i>	25.53

noisy and noiseless coefficient under zero-mean noise with variance τ^2 . Thus, the overall procedure is similar to the Wiener filter in Similarity Domain [20] but uses $\mathcal{T}_{1D}(\tilde{\mathbf{g}}_k^{(j)})$ both as the pilot and as the noisy coefficient to be shrunk.

IV. EXPERIMENTS

We evaluated NN3D over several datasets: 'Set12', 'BSD68' and 'Urban100' [21]. We have chosen three state-of-the-art CNNF for AWGN removal: DnCNN [11], WDnCNN [15] and FFDNet [18], both for the comparison and as the CNNF module of NN3D, where they are used without any modification or re-training. For all experiments, our implementation of NN3D uses $K=2$, $\lambda_k=k^{-1}$, $\tau_k=\frac{1}{4}\sigma\lambda_k$, $N_1=10$, $N_2=32$, and \mathcal{T}_{1D} is the Haar wavelet transform.

Because the noise variance in \tilde{z}_k is approximately $\lambda_k^2\sigma^2$, the CNNF has to be able to operate at different noise levels. However, some CNNFs (see, e.g., [10], [11]) entail models trained for specific noise standard deviation values $\Sigma=\{\sigma_1, \dots, \sigma_M\}$. Of the three CNNFs under analysis, FFDNet was trained for noise of arbitrary strength: $\Sigma=[0, 75]$, whereas the other two were trained for specific noise levels: $\Sigma=\{5:5:75\}$ for DnCNN, and $\Sigma=\{15, 30, 50\}$ for WDnCNN. We thus filter \tilde{z}_k upon scaling it by a factor α_k , which is selected so that the standard deviation of $\alpha_k\tilde{z}_k$, i.e. $\alpha_k\lambda_k\sigma$, matches one of the standard-deviation levels Σ the CNN has been trained for. In practice α_k should not deviate too much from 1, otherwise $\alpha_k\tilde{z}_k$ will not fit the dynamic range of the training images, and, when $\alpha_k > 1$, $\alpha_k\tilde{z}_k$ may even exceed the range adopted for processing, negatively impacting the performance of the overall scheme. Hence we set $\alpha_k = \lambda_k^{-1}\sigma^{-1}\varsigma_k$, where $\varsigma_k = \max\{\{\varsigma \in \Sigma \mid \varsigma \leq \lambda_k\sigma\} \cup \min \Sigma\}$ and Line 3 of Algorithm 1 becomes $\tilde{y}_k = \alpha_k^{-1}\text{CNNF}(\alpha_k\tilde{z}_k, \varsigma_k)$.

Table I reports peak signal to noise ratio (PSNR) results of the evaluated methods. For stronger noise, NN3D noticeably outperforms the state-of-the-art methods. Maximal gain over the adopted CNNF modules is achieved on images having strong self-similarity, such as those from the set 'Urban100'.

In Fig. 2 one can see that BM3D outperforms WDnCNN on 'Barbara', while WDnCNN outperforms BM3D on 'House' and 'Starfish'. However, in all three instances, our approach outperforms BM3D and WDnCNN, numerically and visually. In 'Starfish', NN3D is able to produce sharper results than both WDnCNN and BM3D, showing that the proposed filter

cascade is able to significantly exceed its building blocks. The results in the table are also better than those obtained by other proposals combining nonlocal processing and CNNs [16], [17]. In [16], 26.07 dB is reported when processing 'BSD68' with $\sigma=50$, a value which is below all of our tested combinations. As for [17], processing 'House' and 'Barbara' with $\sigma=50$ results in 30.25 dB and 26.84 dB respectively, values which are also significantly below our best results reported in Fig. 2.

As mentioned in Section III-A, the effectiveness of BM can be seriously compromised if this were applied on a noisy image; in particular, if BM is applied directly on z instead of on \tilde{y}_1 , the average PSNR loss over the experiments reported in Table I ranges from approximately 0.1 dB when $\sigma=30$ to 0.6 dB when $\sigma=75$. Nonetheless, the proposed framework is generic enough that BM can be performed on the estimate of y provided by another filter. For instance, we observed that the results obtained by performing BM on an estimate provided by BM3D are equivalent to the ones presented in this section, both visually and quantitatively (within 0.05 dB from the average PSNRs reported in Table I).

These experiments were conducted on a computer running Ubuntu 16.04 LTS, equipped with an AMD Ryzen Threadripper 1950X CPU and an Asus GeForce GTX 1080 Ti 11GB Turbo GPU. When processing a 256×256 image, we observed the following average execution times for a single call of each module. Running single threaded on CPU: BM 0.10 s; NLF 0.11 s. Running on CPU + GPU: DnCNN 0.06 s; FFDNet 0.04 s; WDnCNN 0.42 s. A complete execution of NN3D ($K=2$) requires the execution of the following modules: CNNF, BM, NLF, CNNF, NLF. The NN3D code used for these experiments can be downloaded from <http://www.cs.tut.fi/sgn/imaging/nn3d>.

V. DISCUSSION AND CONCLUSION

Even though the receptive fields (a.k.a. field of view) of the analyzed CNNs are in principle large enough to capture non-local self-similarity (35×35 for DnCNN, 62×62 for FFDNet, 82×82 for WDnCNN, vs. 39×39 search neighborhood of the BM in NN3D), their distribution of impact follows a Gaussian distribution, meaning that the *effective* receptive field of this type of deep CNNs is significantly narrower [22]. Pixels at the center of the field contribute much more than those towards the

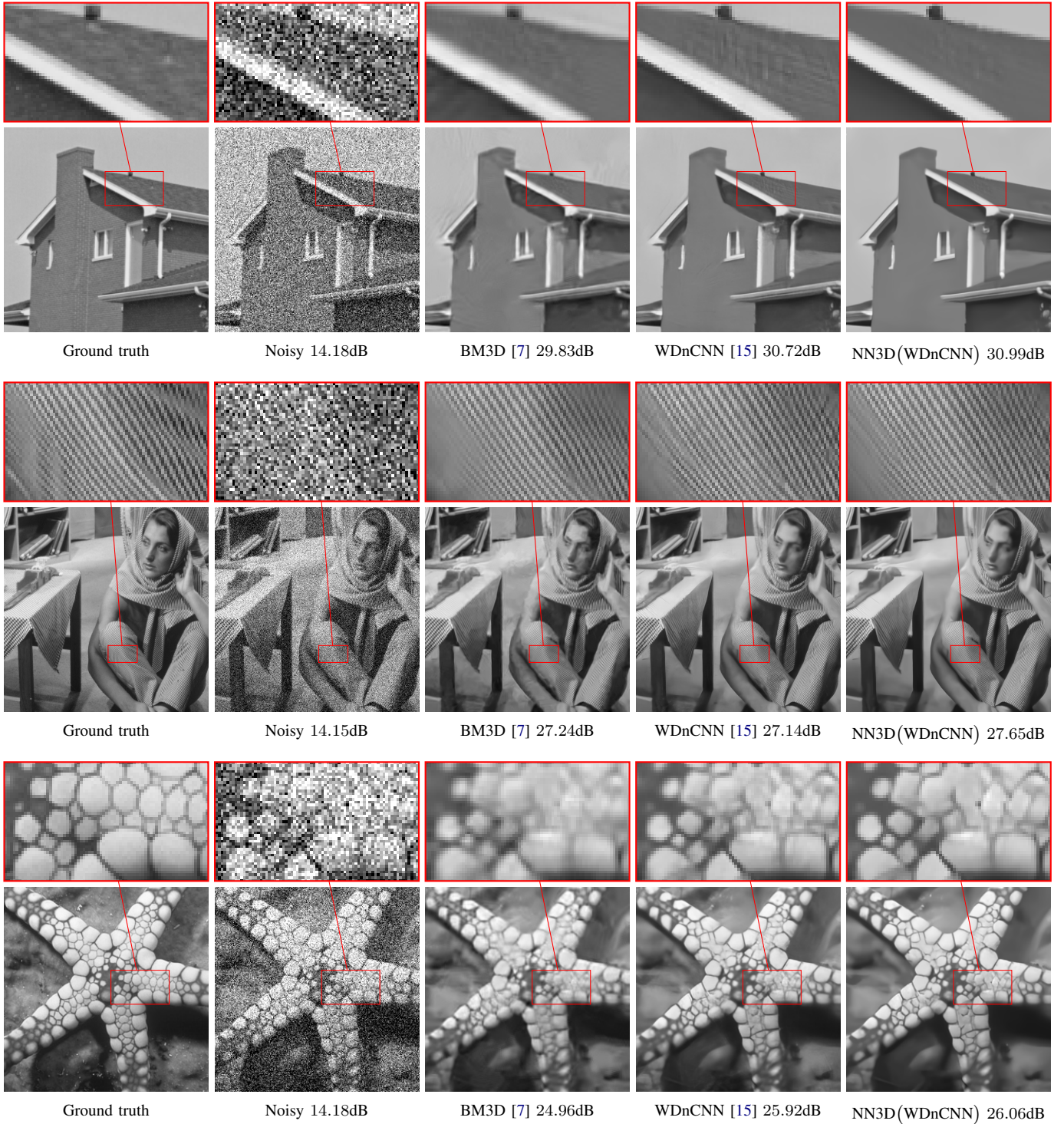


Fig. 2. House, Barbara, and Starfish, from *Set12*, with $\sigma=50$, processed by different methods with respective PSNR.

periphery. Furthermore, the effective receptive field grows with the square root of the depth of the network. This factor alone explains why these networks are strongly biased towards local features and why the inclusion of a nonlocal element results in a dramatic performance improvement.

We showed that the proposed filter cascade is able to boost the performance of current state-of-the-art CNMF. This is achieved in part by mitigating hallucinations introduced by

CNMF, especially when dealing with higher noise variance. This type of artifacts violate the self-similarity prior and are therefore attenuated by the NLF. Overall, the proposed approach yields cleaner images with much sharper reconstruction of details.

Finally, the modular nature of the proposed framework allows for the use of whichever NLF best integrates with the CNMF, processing environment, and data at hand.

REFERENCES

- [1] P. Milanfar, "A tour of modern image filtering: New insights and methods, both practical and theoretical," *IEEE Signal Processing Magazine*, vol. 30, no. 1, pp. 106–128, Jan 2013.
- [2] A. Foi, V. Katkovnik, and K. Egiazarian, "Pointwise shape-adaptive DCT for high-quality denoising and de-blocking of grayscale and color images," *IEEE Transactions on Image Processing*, vol. 16, no. 5, pp. 1395–1411, May 2007.
- [3] S. H. Chan, X. Wang, and O. A. Elgendy, "Plug-and-play ADMM for image restoration: Fixed-point convergence and applications," *IEEE Transactions on Computational Imaging*, vol. 3, no. 1, pp. 84–98, March 2017.
- [4] F. Heide, M. Steinberger, Y.-T. Tsai, M. Rouf, D. Pajak, D. Reddy, O. Gallo, J. Liu, W. Heidrich, K. Egiazarian, J. Kautz, and K. Pulli, "FlexISP: A flexible camera image processing framework," *ACM Trans. Graph.*, vol. 33, no. 6, pp. 231:1–231:13, Nov. 2014. [Online]. Available: <http://doi.acm.org/10.1145/2661229.2661260>
- [5] K. Zhang, W. Zuo, S. Gu, and L. Zhang, "Learning deep CNN denoiser prior for image restoration," in *2017 IEEE Conference on Computer Vision and Pattern Recognition (CVPR)*, July 2017, pp. 2808–2817.
- [6] M. Lebrun, A. Buades, and J.-M. Morel, "Implementation of the "Non-Local Bayes" (NL-Bayes) Image Denoising Algorithm," *Image Processing On Line*, vol. 3, pp. 1–42, 2013.
- [7] K. Dabov, A. Foi, V. Katkovnik, and K. Egiazarian, "Image denoising by sparse 3-D transform-domain collaborative filtering," *IEEE Transactions on Image Processing*, vol. 16, no. 8, pp. 2080–2095, Aug 2007.
- [8] V. Katkovnik, A. Foi, K. Egiazarian, and J. Astola, "From local kernel to nonlocal multiple-model image denoising," *International Journal of Computer Vision*, vol. 86, no. 1, p. 1, Jul 2009. [Online]. Available: <https://doi.org/10.1007/s11263-009-0272-7>
- [9] S. Gu, Q. Xie, D. Meng, W. Zuo, X. Feng, and L. Zhang, "Weighted nuclear norm minimization and its applications to low level vision," *International Journal of Computer Vision*, vol. 121, no. 2, pp. 183–208, Jan 2017. [Online]. Available: <https://doi.org/10.1007/s11263-016-0930-5>
- [10] Y. Chen and T. Pock, "Trainable nonlinear reaction diffusion: A flexible framework for fast and effective image restoration," *IEEE Transactions on Pattern Analysis and Machine Intelligence*, vol. 39, no. 6, pp. 1256–1272, June 2017.
- [11] K. Zhang, W. Zuo, Y. Chen, D. Meng, and L. Zhang, "Beyond a Gaussian denoiser: Residual learning of deep CNN for image denoising," *IEEE Transactions on Image Processing*, vol. 26, no. 7, pp. 3142–3155, July 2017.
- [12] I. Mosseri, M. Zontak, and M. Irani, "Combining the power of internal and external denoising," in *2013 IEEE International Conference on Computational Photography (ICCP)*. IEEE, 2013, pp. 1–9.
- [13] M. Ebrahimi and E. R. Vrscay, "Examining the role of scale in the context of the non-local-means filter," in *International Conference Image Analysis and Recognition*. Springer, 2008, pp. 170–181.
- [14] M. Zontak, I. Mosseri, and M. Irani, "Separating signal from noise using patch recurrence across scales," in *Proceedings of the IEEE Conference on Computer Vision and Pattern Recognition*, 2013, pp. 1195–1202.
- [15] W. Bae, J. J. Yoo, and J. C. Ye, "Beyond deep residual learning for image restoration: Persistent homology-guided manifold simplification," *CoRR*, vol. abs/1611.06345, 2016. [Online]. Available: <http://arxiv.org/abs/1611.06345>
- [16] S. Lefkimmatis, "Non-local color image denoising with convolutional neural networks," in *2017 IEEE Conference on Computer Vision and Pattern Recognition (CVPR)*, July 2017, pp. 5882–5891.
- [17] B. Ahn and N. I. Cho, "Block-matching convolutional neural network for image denoising," *CoRR*, vol. abs/1704.00524, 2017. [Online]. Available: <http://arxiv.org/abs/1704.00524>
- [18] K. Zhang, W. Zuo, and L. Zhang, "FFDNet: Toward a fast and flexible solution for CNN based image denoising," *CoRR*, vol. abs/1710.04026, 2017. [Online]. Available: <http://arxiv.org/abs/1710.04026>
- [19] H.-Y. Gao and A. G. Bruce, "Waveshrink with firm shrinkage," *Statistica Sinica*, pp. 855–874, 1997.
- [20] C. Cruz, R. Mehta, V. Katkovnik, and K. Egiazarian, "Single image super-resolution based on Wiener filter in similarity domain," *IEEE Transactions on Image Processing*, vol. PP, no. 99, pp. 1–1, 2017.
- [21] <https://github.com/iorism/CNN/tree/master/testsets>, accessed: 2018-02-26.
- [22] W. Luo, Y. Li, R. Urtasun, and R. Zemel, "Understanding the effective receptive field in deep convolutional neural networks," in *Advances in Neural Information Processing Systems 29*, D. D. Lee, M. Sugiyama, U. V. Luxburg, I. Guyon, and R. Garnett, Eds. Curran Associates, Inc., 2016, pp. 4898–4906.